Enzyme Structures

DOI: 10.1002/ange.201105241

Inferential NMR/X-ray-Based Structure Determination of a Dibenzo[*a*,*d*]cycloheptenone Inhibitor–p38α MAP Kinase Complex in Solution**

Valerie S. Honndorf, Nicolas Coudevylle, Stefan Laufer, Stefan Becker, Christian Griesinger, and Michael Habeck**

The adenosine triphosphate (ATP) binding site of the p38 mitogen-activated protein kinase (MAPK) undergoes a large conformational change during its catalytic cycle. Compounds that target the active site, such as the pyridinyl-imidazole SB203580 and 4-phenylaminodiarylketones,[1,2] have been shown to bind to p38 MAPK with a high affinity but a low specificity as a result of the high conformational flexibility of these compounds. Increasing the rigidity of small-molecule inhibitors should, therefore, improve the specificity of binding to p38 MAPK.[3] This led to the development of tricyclic dibenzo[*a*,*d*]cycloheptenone and dibenzo[*b*,*e*]oxepinone inhibitors,[3] which contain condensed ring systems that stabilize the molecular geometry.

The crystal structure of p38α MAPK in complex with the tricyclic inhibitor 2-(2-aminophenylamino)-10,11-dihydrodibenzo[*a*,*d*]cyclohepten-5-one[3] (**1**, Figure S1 in the Supporting Information) has been determined by Koeberle et al.[4] at 1.85 Å resolution. Because crystal structures, especially of kinase complexes, may not reflect the conformation of the kinase in solution,[5] we used NMR spectroscopy to study the binding mode of **1** to p38α in solution at ambient temperature. We measured TROSY spectra of deuterated p38α in complex with **1** (p38α–**1**, $IC_{50} = 104$ nM) and assigned 62% of the detected resonances. The TROSY-HSQC spectrum of free p38α has about 75% of the expected signals, which confirms previous studies.[5,6] Comparison of the spectra of free p38α and p38α–**1** reveals chemical shift perturbations at the binding site of the inhibitor. Compound **1** is located in the hydrophobic back pocket and forms hydrogen bonds to the hinge region.[4] Upon binding of **1**, the resonances of most of the amino acids that are involved in these contacts disappear as a result of line broadening, which indicates that several conformations are in intermediate exchange; the glycine-rich loop is partly affected in the same way.

Figure 1 A shows an overlay of the TROSY-HN(CO) spectra of free p38α and p38α–**1**, which are sequentially labeled with ^{13}C and ^{15}N-Leu/^{15}N-Met (see also Figure S2 in the Supporting Information). After the addition of **1**, the cross-peaks between Leu108–Met109 and Leu86–Leu87 are no longer detected. TROSY-HSQC spectra with ^{13}C and ^{15}N-His/^{15}N-Leu-labeling give similar results (Figure 1 B). Upon binding of **1**, the signals from the hinge region that connects the N lobe and the C lobe (His107, Leu108) as well as signals from the hydrophobic pocket (Leu86, Leu87) disappear, whereas amino acids that are distant from the binding pocket (Leu164 and His142 in the C lobe and His80 in the N lobe) have perturbed chemical shifts. From the disappearance of the signals we conclude that the motion on the intermediate-exchange timescale (μs–ms) is present in p38α–**1** and is similar to that in the p38α–SB203580 complex.[5] This is particularly remarkable because SB203580 and **1** are structurally unrelated. Thus, the complex is more dynamic in the binding site than the free kinase for both flexible SB203580 and rigid **1**.

To characterize the solution structure of the kinase–inhibitor complex, we measured ^{1}H–^{15}N residual dipolar couplings (RDCs), which are sensitive probes of the orientation of the backbone. 58 RDCs that ranged from −40 to +50 Hz with acceptable errors (< 5 Hz) were considered for further analysis. We compared the RDCs of free p38α and p38α–**1** without reference to a structure (Figure S3 in the Supporting Information) and found that many of the couplings are very similar. This is an indication that the solution structure of p38α–**1** resembles the free form in large parts (Figure S3 in the Supporting Information). The most prominent discrepancies are found for Gly33 and Gly36 in the glycine-rich loop (−34 and −26 Hz in the complex versus −9.1 and −0.3 Hz in the free form, respectively, Table 1). Comparison of the N–H orientations derived from free and bound p38α RDCs indicates that some of the N–H bonds rotate during the formation of the complex. Among the residues for which RDCs could be measured, Gly33 and Gly36, which are

[*] Dr. V. S. Honndorf,[+] Dr. N. Coudevylle,[+] Dr. S. Becker, Prof. Dr. C. Griesinger
Department of NMR-based Structural Biology
Max Planck Institute for Biophysical Chemistry
Am Fassberg 11, 37077 Göttingen (Germany)
E-mail: cigr@nmr.mpibpc.mpg.de
Dr. M. Habeck
Department of Protein Evolution
Max Planck Institute for Developmental Biology
Spemannstrasse 35, 72076 Tübingen (Germany)
E-mail: michael.habeck@tuebingen.mpg.de
Prof. Dr. S. Laufer
Department of Pharmaceutical and Medicinal Chemistry
Institute of Pharmacy, Eberhard-Karls-University
Tübingen (Germany)

[+] These authors contributed equally.

[**] M.H. acknowledges funding from the German Science Foundation (DFG HA 5918/1-1). C.G. thanks the Max Planck Society and the DFG (GRK 1034). We thank Thilo Stehle and Johannes Romir for providing the crystal structure and X-ray data for the p38α–**1** complex.

Supporting information for this article is available on the WWW under http://dx.doi.org/10.1002/anie.201105241.

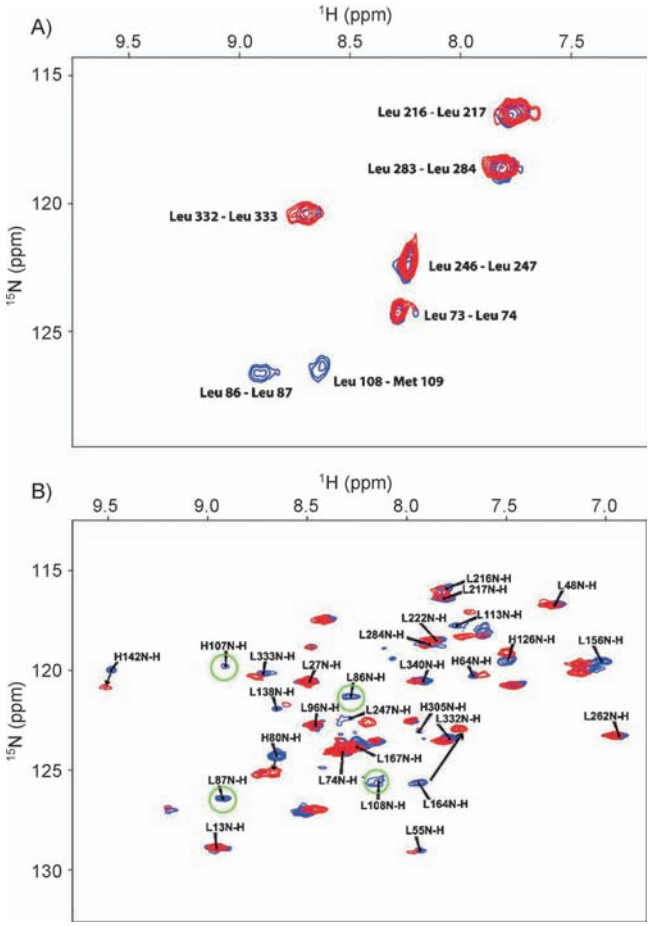

Figure 1. A) Overlay of 2D HNCO spectra of free p38α (blue) and p38α–**1** (red). The samples are labeled with ^{13}C and ^{15}N-Leu/^{15}N-Met. B) Overlay of the 2D ^{1}H-^{15}N TROSY-HSQC spectra that were acquired with selectively labeled ^{13}C,^{15}N-His/^{15}N-Leu samples. Blue: p38α; red: p38α–**1**.

Table 1: Experimental RDCs for Gly33 and Gly36 in p38α and p38α–**1** and the back-calculated couplings (in Hz) for the structures of the complex. The bottom rows shows R_{work} and R_{free} that are derived from the NMR spectra and the X-ray crystal structure.

	Exp. p38α	Exp. p38α–**1**	1P38	1P38 RDC refined	p38α–**1** crystal	p38α–**1** hybrid initial	p38α–**1** hybrid final
G33	−9.1	−34	−4.3	−33.2	−13.8	−27.4	−31.7
G36	−0.3	−26	11	−26.3	32.8	−20.7	−23
CC	–	–	0.87	0.999	0.787	0.965	0.995
Q	–	–	0.52	0.03	0.557	0.16	0.062
R_{work}	–	–	0.48	0.5	0.177	0.28	0.225
R_{free}	–	–	0.49	0.49	0.227	0.30	0.254

part of the glycine-rich loop, show the largest reorientations (Figure S4 in the Supporting Information).

The fit between the crystal structure of free p38α (1P38) and the RDCs of p38α–**1** is relatively poor (correlation coefficient (CC) = 0.87, Q-factor (Q) = 0.52). The fit was improved by simultaneous refinement of 1P38 against the RDCs and positional restraints that restrict the conformational sampling to the vicinity of the original structure. When applying a relatively strong force, the fit becomes perfect within a few refinement steps (CC = 1.0, Q = 0.03). The largest structural changes occur in the glycine-rich loop and indicate a loop-closure motion (Figure 2 and movie in the Supporting Information).

To investigate if there is an inherent difference between the crystal and solution structures in more detail, we back-calculated the 58 couplings from the crystal structure of p38α–**1**[4] and obtained a fit (CC = 0.787, Q = 0.557) that was even worse than for the crystal structure of free p38α. However, an analysis of 138 known p38α structures in the Protein Data Bank (PDB) produced only slightly better fits, in which the Q value never drops below 0.39 (Figure S5 in the Supporting Information). Similar results were obtained when the anisotropic parameters were fitted against crystal structures of smaller globular proteins, such as ubiquitin.[7]

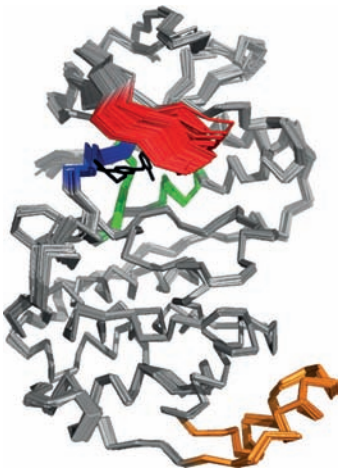

Figure 2. Ensemble that results from flexible fitting of 1P38 against the dipolar couplings of p38α–**1**. The inhibitor (black) is shown in its conformation in the crystal structure of p38α–**1** from Ref. [4]. Red: glycine-rich loop (residues 30–37); blue: hinge region (residues 106–110); green: hydrophobic back pocket (residues 72–77 and 83–87); orange: C lobe residues that have the largest difference between the crystal and the hybrid structures of p38α–**1** (residues 240–265, see Figure 4A).

To test if the crystal structure of p38α–**1** can be reconciled with the NMR data, we refined the crystal structure of p38α–**1** against the dipolar couplings by using the ISD software package.[8,9] As well as the RDC restraints, positional restraints were introduced to mimic an R factor from the X-ray crystal structure. Each positional restraint was weighted by its inverse B factor to allow mobile atoms to move more freely during refinement. Figure 3A shows that the positional restraint energy correlates strongly with the crystallographic R factors (R_{work} = 1.00, R_{free} = 0.97). Joint refinement against the positional and RDC restraints results in a hybrid structure (PDB ID = 2lgc) that fits both the X-ray crystal structure and the NMR spectra. Figure 3B shows the joint evolution of the restraint energies in the first round of refinement. The initial structure fits the NMR data well but has poor R factors (CC = 0.965, Q = 0.16, R_{work} = 0.28, R_{free} = 0.30). During refinement, the X-ray energy improves initially, whereas the fit to the

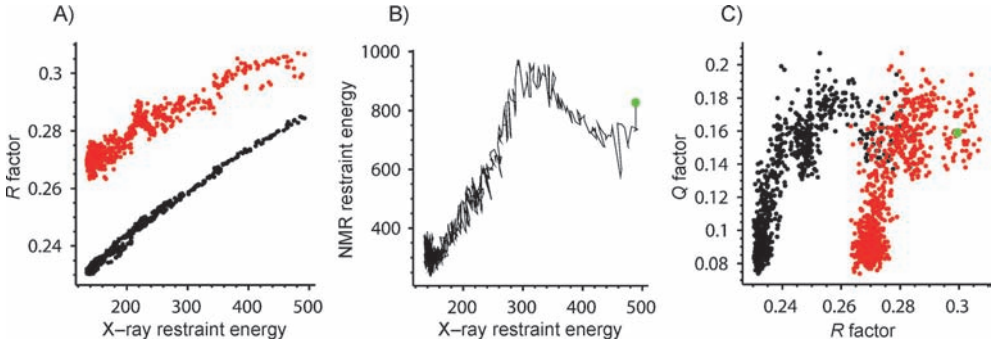

Figure 3. Joint X-ray/NMR refinement and development of quality factors. A) Correlation between *R* factors and X-ray energy. Black: R_{work}; red: R_{free}. B) Joint optimization of the restraint energy from the X-ray crystal structure and NMR spectra. C) Correlation between crystallographic *R* factors and the NMR *Q* factor. Black: R_{work}; red: R_{free}. The green dot in panels (B) and (C) indicates the initial structure.

couplings deteriorates, which is reflected in an increase in the NMR restraint energy. After 100 iterations, the refinement found a conformation that can be optimized jointly over both energies (Figure 3 C). A second round of refinement based on the NMR/X-ray data yielded a set of slightly different structures with both favorable *Q* and *R* factors (Figure S6 in the Supporting Information). The structure with best R_{free} has CC = 0.995, $Q = 0.062$, $R_{work} = 0.225$, and $R_{free} = 0.254$. Note that for the initial structure, the quality factors that are derived from both NMR and X-ray data were worse than for the final hybrid structure (Table 1). The *R* values of the hybrid structure are within the expected range (Figure S7 in the Supporting Information). The RDC *Q* value of the final hybrid structure is very low, whereas R_{free} is slightly higher relative to the crystal structure. By weighting the restraints from the NMR spectra and the X-ray crystal structure differently, R_{free} was improved further, thereby shifting the *Q* factor to more realistic values (see Figure S9 in the Supporting Information), but this does not change the structure significantly. The Ramachandran plot of both structures is consistent (Figures S10–S15 in the Supporting Information); the hybrid structure has a more regular conformation, as indicated by the Procheck *G* factor. We conclude that, despite minor differences, crystallographic and RDC data can be explained with the same structure.

We compared the crystal structure of p38α–**1** with the hybrid NMR/X-ray structure to pinpoint possible differences. The overall root mean square deviation (RMSD) between the two structures is 0.22 Å and 0.67 Å for the α carbon atoms and all non-hydrogen atoms, respectively. The core of both structures is virtually identical, and the largest differences are found in the C lobe (Figure 4 A highlights the regions with the largest differences), which is distant from where the inhibitor binds. There is a good correlation ($r = 0.84$) between the *B* factors and the local RMSD (Figure 4 B) in the crystal and hybrid structures of p38α–**1**. This is somewhat expected because positional restraints are weighted by their inverse *B* factors during refinement. Another interesting correlation is noted for the difference between the measured and back-calculated RDCs when compared between the crystal and the hybrid structures (Figure S8 in the Supporting Information). The correlation ($r = 0.70$) indicates that the mismatch between experimental and back-calculated couplings is consistent across both structures, yet is scaled by more than a factor of five. Among the couplings that have the largest mismatches are Gly33 and Gly36 (Table 1 and Figure 4 C). However the remaining discrepancies are negligible because they drop from 20 and 58 Hz to 2.3 and 3 Hz, respectively, during refinement, which is within the experimental

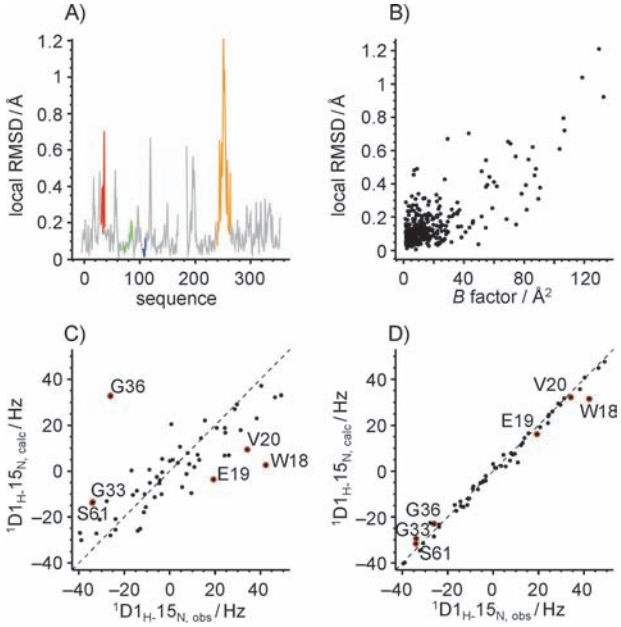

Figure 4. A) Local RMSD between the crystal and hybrid structures of p38α–**1**. Red: glycine-rich loop; blue: hinge region; green: hydrophobic pocket; orange: C lobe residues. B) Correlation between the *B* factor and local RMSD. C) Dipolar couplings of p38α–**1** fitted with the X-ray crystal structure (amino acids with mismatch > 20 Hz are highlighted in red, the values for Gly33 and Ser61 are very similar and overlap in the figure). D) Dipolar couplings for the hybrid structure (the same amino acids are highlighted as in panel C)).

error of the couplings. The remaining mismatch at Gly33 and Gly36 may be partly due to mobility. The two glycine residues are located in the glycine-rich loop, which is quite mobile in the crystal structure. The amide groups of Gly33 and Gly36 have elevated *B* factors of 55.5 Å^2 and 37.1 Å^2, respectively. However, this was not further investigated because a more detailed analysis would require RDC data from multiple alignment media.

In conclusion, data from NMR spectroscopy show an interaction between **1** and p38α in solution and a structural change in the ATP binding pocket of p38α when binding to **1**. This change is consistent with the structural changes in the

crystal structures of free p38α and p38α–**1**. By using inferential X-ray/NMR-based structure determination, we find that the crystal structure of the complex is very close to the hybrid structure, which is compatible with both the crystal structure and the data from NMR experiments in solution. However, the unrefined crystal structure does not fulfill the solution data well, which may be a result of structural noise (RDCs are very sensitive to orientations, whereas X-ray data are not) or differences caused by crystal packing. We expect that the joint refinement of sparse NMR data and X-ray crystallography data will be useful for many systems when checking whether crystal structures and the main conformation in solution are the same.

Experimental Section

Sample preparation: Single amino acid labeling and purification of human p38α was carried out as previously described[10,11] with minor modifications. Inhibitors were prepared in [D_6]DMSO at a concentration of 50 mM and added to the protein sample (0.5–1.0 mM) in a 2:1 and 1:1 ratio.

NMR spectroscopy: NMR experiments were carried out at 298 K on Bruker Avance spectrometers equipped with *z*-gradient cryoprobes operating at 400, 600, and 800 MHz. All NMR spectra were processed by using NMRPipe/NMRDraw[12] and Xwinnmr (Bruker). NMR spectra were analyzed by using Sparky (http://www.cgl.ucsf.edu/home/sparky/) and CARA.[13] The resonances of the inhibitor were assigned by recording ^{13}C–^{1}H HSQC, HMBC, COSY, and NOESY spectra. Assignment of the resonances in the ^{1}H NMR ^{15}N NMR, and ^{13}C NMR spectra of p38α were taken from Biological Magnetic Resonance Data Bank (BMRB) entry bmr6468.[14] Backbone amide resonances of p38α–**1** were assigned by using ^{1}H-^{15}N TROSY-HSQC, TROSY-HNCA, and TROSY-HN(CO) spectra that were recorded for a triple labeled sample (^{2}D, ^{13}C, and ^{15}N) or specifically labeled samples. RDCs were measured on a double labeled sample (^{2}D and ^{15}N) in a partially aligned medium by using the bacteriophage Pf1 (Profos) at a concentration of 20 mg mL^{-1} at pH 6, which provides a splitting of 12.76 Hz for the D_2O signal. One-bond $^{1}J_{1H-15N}$ and residual $^{1}D_{1H-15N}$ couplings were measured in ^{1}H-^{15}N HSQC and ^{1}H-^{15}N TROSY-HSQC spectra of p38α and p38α–**1**.

Received: July 26, 2011
Revised: December 23, 2011
Published online: January 24, 2012

Keywords: dibenzo[*a*,*d*]cycloheptenones · kinases · NMR spectroscopy · structure elucidation · X-ray diffraction

[1] E. R. Ottosen, M. D. Sorensen, F. Bjorkling, T. Skak-Nielsen, M. S. Fjording, H. Aaes, L. Binderup, *J. Med. Chem.* **2003**, *46*, 5651 – 5662.
[2] L. Revesz, E. Blum, F. E. Di Padova, T. Buhl, R. Feifel, H. Gram, P. Hiestand, U. Manning, G. Rucklin, *Bioorg. Med. Chem. Lett.* **2004**, *14*, 3601 – 3605.
[3] S. A. Laufer, G. M. Ahrens, S. C. Karcher, J. S. Hering, R. Niess, *J. Med. Chem.* **2006**, *49*, 7912 – 7915.
[4] S. C. Koeberle, J. Romir, S. Fischer, A. Koeberle, V. Schattel, W. Albrecht, C. Grütter, O. Werz, D. Rauh, T. Stehle, S. A. Laufer, *Nat. Chem. Biol.* **2011**, doi: 10.1038/nchembio.761 [Epub ahead of print].
[5] V. S. Honndorf, N. Coudevylle, S. Laufer, S. Becker, C. Griesinger, *Angew. Chem.* **2008**, *120*, 3604 – 3607; *Angew. Chem. Int. Ed.* **2008**, *47*, 3548 – 3551.
[6] M. Vogtherr, K. Saxena, S. Hoelder, S. Grimme, M. Betz, U. Schieborr, B. Pescatore, M. Robin, L. Delarbre, T. Langer, K. U. Wendt, H. Schwalbe, *Angew. Chem.* **2006**, *118*, 1008 – 1012; *Angew. Chem. Int. Ed.* **2006**, *45*, 993 – 997.
[7] G. Cornilescu, J. L. Marquardt, M. Ottiger, A. Bax, *J. Am. Chem. Soc.* **1998**, *120*, 6836 – 6837.
[8] W. Rieping, M. Habeck, M. Nilges, *Science* **2005**, *309*, 303 – 306.
[9] W. Rieping, M. Nilges, M. Habeck, *Bioinformatics* **2008**, *24*, 1104 – 1105.
[10] D. M. Lemaster, F. M. Richards, *Biochemistry* **1988**, *27*, 142 – 150.
[11] M. Bukhtiyarova, K. Northrop, X. Chai, D. Casper, M. Karpusas, E. Springman, *Protein Expression Purif.* **2004**, *37*, 154 – 161.
[12] F. Delaglio, S. Grzesiek, G. W. Vuister, G. Zhu, J. Pfeifer, A. Bax, *J. Biomol. NMR* **1995**, *6*, 277 – 293.
[13] R. Keller, *The Computer Aided Resonance Assignment Tutorial*, Cantina Verlag, Goldau, **2004**.
[14] M. Vogtherr, K. Saxena, S. Grimme, M. Betz, U. Schieborr, B. Pescatore, T. Langer, H. Schwalbe, *J. Biomol. NMR* **2005**, *32*, 175.

